EFFECTS OF EIGHT PHOTOVOLTAIC MOUNTING SYSTEMS ON THE GROWTH PERFORMANCE OF SALICORNIA HERBARIA AND SOIL PARAMETERS IN SALINE-ALKALI SOILS

光伏场 8 种支架模式对盐碱地碱蓬群落生长性能和土壤指标的影响

Nannan MA[1)], Shanmin QU[1*)], Feng WANG[1)], Tongtong LI [1)], Yueming LI[1)], Junde ZHOU[1)]
College of Animal Science and Technology, Heilongjiang Bayi Agricultural University, Daqing/ China
Tel: +8613936730023; E-mail: 64311742@qq.com
Corresponding author: Shanmin Qu
DOI: https://doi.org/10.35633/inmateh-78-55

Keywords: *photovoltaic support structure model, Salicornia herbacea, saline-alkali land, soil properties*

ABSTRACT
This study aims to systematically evaluate the effects of eight distinct photovoltaic mounting systems at the National Photovoltaic Energy Storage Demonstration Platform on the growth performance of Suaeda glauca and soil properties in saline–alkali land. The results showed that the dual-axis tracking support system between panels (SJ) significantly outperformed the other treatments (P<0.05), achieving the highest plant height (36.20 cm), stem diameter (1.84 mm), and leaf width (2.11 mm), as well as higher dry matter accumulation and fresh biomass. In addition, this system exhibited the highest total potassium content (44.36 mg/kg) and the highest D-value (1.30) based on comprehensive membership function evaluation. The application of the dual-axis tracking support system enhances the yield of Suaeda glauca and promotes soil organic matter recovery, thereby achieving the dual objectives of improving photovoltaic system productivity and supporting ecological restoration of halophytic vegetation.

摘要
本研究旨在系统评估国家光伏储能实证实验平台 8 种不同光伏支架模式对盐碱地先锋植物碱蓬（Suaeda glauca）群落生长性能及土壤特性的影响。采用随机区组设计，测定光伏阵列板间、板下、非光伏区场内、场外对照组碱蓬植株高度、盖度等形态指标，并采集 0–20 cm 土层样本测定 pH、电导率、养分等含量。结果表明，双轴跟踪支架板间（SJ）在植株高度（36.20 cm）、茎粗（1.84 mm）和叶宽（2.11 mm）上显著优于其他处理（P<0.05），干重、鲜重亦居高位；双轴跟踪支架全钾最高（44.36 mg/kg）。双轴跟踪支架综合隶属函数评价 D 值最高（1.30），表明双轴跟踪支架对草地生态系统正向影响最显著。在盐碱草地开展光伏 -农业协同利用时，优先选用双轴跟踪支架模式，可提升碱蓬产量并促进土壤有机质恢复，实现光伏系统与盐生植被的协同增产与生态修复双重目标。

INTRODUCTION

In recent years, renewable energy sources have seen widespread adoption globally, encompassing diverse forms such as wind power, solar power, tidal power, and hydropower *(Ravi et al., 2015)*. The primary reason for their prominence lies in their significant advantages in mitigating climate change. Under the dual carbon goals, photovoltaic (PV) power generation has become a pivotal force in China's transition to green energy, owing to its clean, efficient, low-carbon, and stable characteristics *(Che et al., 2025)*. According to the International Renewable Energy Agency (IRENA), global renewable energy capacity additions reached 473 GW in 2023, with solar PV contributing 345.5 GW – accounting for 73% of the total – bringing its cumulative global capacity to 1.42 TW. China stands as the world's largest PV production and installation market. In 2023, the nation's photovoltaic industry achieved remarkable growth, with new annual installations reaching 216.88 GW – a 148% year-on-year increase – fostering diverse application scenarios such as ‘pasture-solar integration,’ ‘fishery-solar integration,’ and ‘agricultural-solar integration’ *(International Report, 2024)*.

[1] *Ma Nannan, MSc in Agriculture; Qu Shanmin, PhD in Agriculture; Wang Feng, MSc in Agriculture; Li Tongtong, MSc in Agriculture; Li Yueming, MSc in Agriculture; Zhou Junde, MSc in Agriculture.*

Saline-alkaline land constitutes a vital reserve of arable resources in China and serves as a crucial ecosystem carrier, rendering its restoration strategically significant *(Amirhossein et al., 2020; Hu et al., 2024)*. Soil salinisation represents one of the major challenges facing global agriculture, limiting crop growth and yield *(Yu et al., 2022)*. Suaeda glauca, a salt-tolerant plant species, possesses unique resilience to extreme conditions and has emerged as a key model plant for studying ecological restoration and agricultural development on saline-alkaline land *(Zhao et al., 2022)*. Suaeda glauca is an annual herb reaching heights of up to 1 metre, featuring a stout, cylindrical stem of pale green colour with prominent ridges and a highly branched apex. Branches are elongated, ascending or descending. Leaves are filiform, semicircular in shape. Flowers are hermaphroditic, solitary or clustered in groups of 2–5, predominantly borne near the leaf base. Capsules are enclosed by petals and covered by a membranous coat. Seeds may grow horizontally or towards the ground. Flowering and fruiting occur from July to September. Grows on saline soils in coastal areas, wastelands, ditch margins, and farmland edges *(Tao et al., 2023)*.

The National Photovoltaic and Energy Storage Demonstration Platform, situated in Datong District, Daqing City, China (124°54′20″N, 46°10′17″E), lies within the Songnen Plain. As China's most northerly high-latitude, high-altitude photovoltaic base, it spans over 100,000 mu (approximately 6,667 hectares), establishing itself as Asia's and indeed the world's largest photovoltaic experimental demonstration base. Inaugurated on 11 August 2021, the platform occupies temperate meadow grassland—a typical degraded saline-alkali grassland where perennial dry grass yields remain between 30–85 kilograms per mu. The effects of different photovoltaic mounting systems on power generation efficiency within the field, and the combined impact of mounting structures and panels on Salicornia communities in Songnen saline-alkali grasslands, remain poorly understood. The interception of precipitation and shading effects from photovoltaic modules alter the intensity of photosynthetically active radiation and soil moisture evaporation processes beneath them, subsequently influencing vegetation characteristics such as cover, plant height, density, uniformity, richness, and biomass *(Wang et ai., 2019)*. Research indicates that photovoltaic power station construction generally favours shade-tolerant plant growth, enhancing vegetation cover and productivity within sites while improving the inherently fragile grassland habitat *(Liu et ai., 2019; Liu et ai., 2022)*. This study aims to elucidate the potential impacts of photovoltaic facilities at the National Photovoltaic and Energy Storage Demonstration Platform (Daqing Base) on Salicornia herbaceum plant communities. Investigating the responses of Salicornia vegetation and soil to photovoltaic panel arrays in saline-alkali soils holds significant theoretical importance for scientifically assessing the effects of photovoltaic power stations on saline-alkali grassland ecosystems. It may also provide decision-making references for the construction of photovoltaic power stations in degraded saline-alkali grassland areas of Northeast China and the future development of grassland photovoltaic industries.

MATERIALS AND METHODS

Study Area Overview

The National Photovoltaic Energy Storage Demonstration Platform (Daqing Base) is situated in Gaotaizi Town, Datong District, Daqing City, Heilongjiang Province, China, at coordinates 124°54′20″ E, 46°10′17″ N. This region represents a transitional zone between grassland and agricultural areas, with the photovoltaic field predominantly located on grassland. The region exhibits a temperate continental monsoon climate characterised by distinct seasons and significant temperature variations. The annual mean temperature is approximately 4.2°C, with extreme maximum temperatures reaching 38.9°C and extreme minimum temperatures dropping to -39.2°C. Annual sunshine hours range between 2600 and 2842 hours, and the high annual total solar radiation provides favourable conditions for solar energy utilisation. Additionally, the region experiences moderate precipitation, with an annual average rainfall of approximately 427.5mm, which is favourable for plant growth and the operation of photovoltaic power stations. The Daqing photovoltaic field area is situated within the low-lying plains of the central Songnen Plain, featuring relatively flat terrain with ground elevations ranging from 129 m to 133 m. The region exhibits relatively uniform topography, predominantly comprising saline-alkali soils with distinctive geological characteristics. Geologically, it lies within the core fault zone of the Songnen Interrupted Depression Belt in the Lesser Khingan Range. The block structure is intact, with minimal neotectonic activity and Holocene fault movement. Seismic intensity remains below VI on the Mercalli scale, classifying it as a geologically stable area. Common vegetation in the test site includes: Suaeda glauca, *Puccinellia tenuiflora, Phragmites australis, Leymus chinensis*, and *Carex rugulosa Kük*.

The National Photovoltaic Energy Storage Demonstration Platform employs eight panel mounting configurations: 1. Flexible fixed mount (R), 2. Flat single-axis tracker (P), 3. Full-dimensional tracker (Q), 4. Seasonally adjustable mount (J), 5. Inclined single-axis tracker (X), 6. Dual-axis tracking mount (S), 7. Vertical single-axis mount (C), 8. Fixed mount (G), 9. Control group—within and outside the PV field (CN, CW) (see Table 1). Data between panels is denoted as J, while data beneath panels is denoted as X. For instance, data between panels on a flexible fixed mount is numbered RJ, and data beneath panels on the same mount is numbered RX.

Table 1

Eight Different Types of Photovoltaic Mounting Systems

Serial No.	Mounting System	Code	Adjustment Angle	Spacing	Key Features	Image
1	Flexible Fixed Mounting	R	Vertical single row, 45° tilt	East-west 19.044m, North-south 8.9m	Pre-stressed cable structure, large span design, strong terrain adaptability	
2	Flat Single-axis Mounting	P	Horizontal axis ±60°, lateral/vertical with 5° or 10° tilt	1.2–1.4m ground clearance, 8–8.8m spacing	East-west tracking with north-south tilt optimisation, 15–25% power output enhancement	
3	Full-Dimensional Tracking Mount	Q	North-south 0°–23°, east-west ±60°	No fixed spacing (requires dynamic avoidance)	Dual-axis tracking (vertical + horizontal), all-weather azimuth/elevation tracking	
4	Seasonally Adjustable Mount	J	Periodic tilt adjustment from 53° to 16° (January-December)	Standard fixed mount spacing	Manual seasonal tilt adjustment, 5%-8% annual power generation increase	
5	Single-axis Tilt Mounting System	X	East-West 45°-135°, Fixed 12°/25° Tilt Angle	East-West 11-15m, North-South 18-23m	Fixed Tilt + Azimuth Tracking, Simple Structure Low Cost	
6	Dual-axis Tracking Mounting System	S	North-South 0° to 70°, East-West -90° to 90°	Lateral 3×4rows horizontally	Vertical axis, horizontal axis tracking solar azimuth and elevation	
7	Vertical Single-Axis Mount	C	0° to +180°	37°, 45° tilt	37°, 45° tilt tracking axis rotates east-west, tracking solar azimuth	
8	Fixed Mount	G	Fixed 40°	Single span ≤30m, typically set at 18m	Lowest cost (0.15-0.3 RMB/W), high stability, but no power generation gain	
9	CK (within/outside site)	CN/CW	Blank control groups set up inside and outside PV site fencing	No grazing or other human disturbance	Ecological comparison experiments to assess fencing enclosure effects on vegetation/soil	

Research Methodology

Selection of Plant Community Types

The Songnen Grassland plant communities exhibit pronounced spatial heterogeneity, with vegetation distributed in patchy patterns or as community complexes. Prior to the construction of the National Photovoltaic Energy Storage Demonstration Platform power station, the grassland in this area had suffered severe degradation due to long-term unregulated grazing. Soil salinisation was pronounced, with some plots exhibiting distinct alkaline patches and sparse vegetation. Based on preliminary field surveys, the *Suaeda* community was selected as the target community type for this study.

Salicornia is an annual succulent halophyte that accumulates salts in its fleshy leaves and secretes salt crystals, significantly reducing surface soil salinity. Its strong shade tolerance enables robust growth under the low-light conditions beneath photovoltaic panels, manifesting as increased leaf width. As a 'pioneer plant' for saline-alkali land remediation, its cultivation markedly enhances soil organic matter and NPK content while exhibiting heavy metal absorption properties.

Plot Sampling Design

Within this study, three distinct conditions (treatments) were established across eight support configurations: complete shading directly beneath photovoltaic panels (PV), unshaded areas between panel rows (Gap), and control zones outside the photovoltaic power station free from panel interference (CK). Within each of these three zones, three relatively independent plots were established within the Salicornia community. Each plot contained one 1 m × 1 m sample square, resulting in 9 treatment combinations. The 8 support types, combined with under-panel and inter-row positions plus the control area inside and outside the field, yielded 18 treatment groups. Each treatment group comprised three 1 m × 1 m sample squares, totalling 9 × 2 × 3 = 54 sample squares. The underlying soil type within the Salicornia community in this study area is saline-alkali soil. Grazing is prohibited in both the photovoltaic panel distribution zone and its internal control area, with no other human disturbances present.

Survey Methodology

A sampling approach was employed in July 2025, involving random sampling between and beneath panels of eight photovoltaic panel types, as well as within and outside the photovoltaic field. First, the latitude, longitude, and altitude of each sample plot were recorded. Subsequently, the total cover of the sample plot was estimated and documented. Concurrently, the total cover of the species community within the sample plot was estimated and recorded. The height of five plants per species within each sample plot was measured (all plants were measured if fewer than five were present), and the average height was calculated. Following the vegetation survey, all aboveground plant parts from each sample plot were collected. These were sorted by plant species, placed into labelled paper envelopes, weighed fresh on-site, and transported to the laboratory. There, they were dried in an oven at a constant temperature of 65°C until constant weight was achieved, with the resulting weight recorded as the dry matter for that plant species.

Stem diameter was measured using a vernier calliper (accuracy 0.01 mm): measure the diameter at the midpoint of the third internode above ground level. Avoid measuring at nodes or scarred areas, ensuring the calliper remains perpendicular to the stem. Leaf width was measured using vernier callipers on fully expanded, healthy leaves, taking the width at the broadest point. Branch number was counted per plant for all primary branches (directly arising from the main stem). Ten plants were sampled per treatment for stem diameter, leaf width with three replicates.

Following completion of the plant community survey, continue within the sample plots to randomly collect three soil cores (0–20 cm depth) using a 5 cm diameter soil auger. These cores will be used to determine soil pH, organic carbon, total nitrogen, total phosphorus, and total potassium content. Soil pH was measured using the potentiometric method; electrical conductivity was determined using a conductivity meter. Total soluble salts in soil were measured using the conductivity method. Soil nutrient determination employed chemical analysis methods: potassium dichromate oxidation for organic matter, Kjeldahl nitrogen determination for total nitrogen, molybdenum-antimony colorimetric method for total phosphorus, and flame photometry for total potassium.

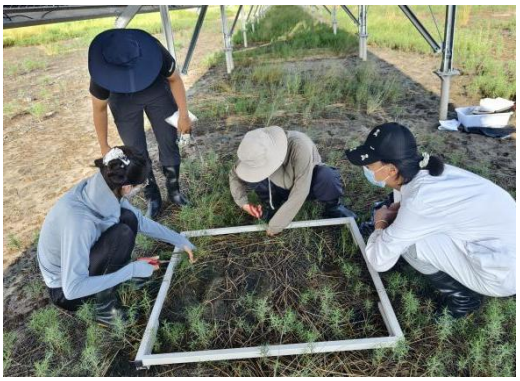

Fig. 1 - Work photographs

Statistical Analysis Methods

The aforementioned data processing was conducted using SPSS 26.0. Bar charts for this study were generated in Origin 2024 and WPS 2021. The data in the chart represent the mean ± standard deviation. Mean comparisons employed the Least Significant Difference (LSD) test for multiple comparisons, with a significance level of $P < 0.05$.

The formulas for calculating the membership function values (W_j), the membership function value $\mu(X_{ja})$, and the composite index evaluation value (D_a) are as follows:

$$W_j = P_j \sum_{i=1}^{n} P_j \quad (1)$$

$$\mu(X_{ja}) = (X_{ja} - X_{jmax}) / (X_{jmin} - X_{jmax}) \quad (2)$$

$$D_a = \sum_{i=1}^{n} [(X_{ja}) \times W_j] \quad (3)$$

In the formula: P_j - Contribution rate of the j-th principal component for each indicator; W_j - Importance level of the j-th principal component among all principal components; X_{ja} - Value of the j-th principal component for the a-th support structure; X_{jmin} - Minimum value of the j-th principal component; X_{jmax} - Maximum value of the j-th principal component; $\mu(X_{ja})$ - membership function value for principal component transformation; D_a - comprehensive evaluation value of the a-th support for national photovoltaic base saltwort grassland vegetation and soil characteristic indicators.

RESULTS

Plant Characteristics of Salicornia Herbaria under Different Support Configurations Effect of Support Configurations on Salicornia Herbaria Height

As illustrated in Fig.2-A, among the eight support configurations, the highest Salicornia height was observed in the double-axis tracking support between panels (SJ), with a community height reaching 36.20 cm. The double-axis tracking support beneath panels (SX) yielded the next highest height at 35.07 cm. while the lowest height was observed between the boards of the inclined single-axis support (XJ), at merely 13.60 cm. Except for the vertical single-axis (C) and inclined single-axis (X) groups, Salicornia communities generally exhibited greater height between the boards (J) than beneath the boards (X). The field control group (CN) showed a significantly higher Salicornia height of 34.40 cm compared to the non-field control group (CW) at 25.71 cm (P<0.05). It is demonstrated that the dual-axis tracking mount has not adversely affected the growth of the saltwort community.

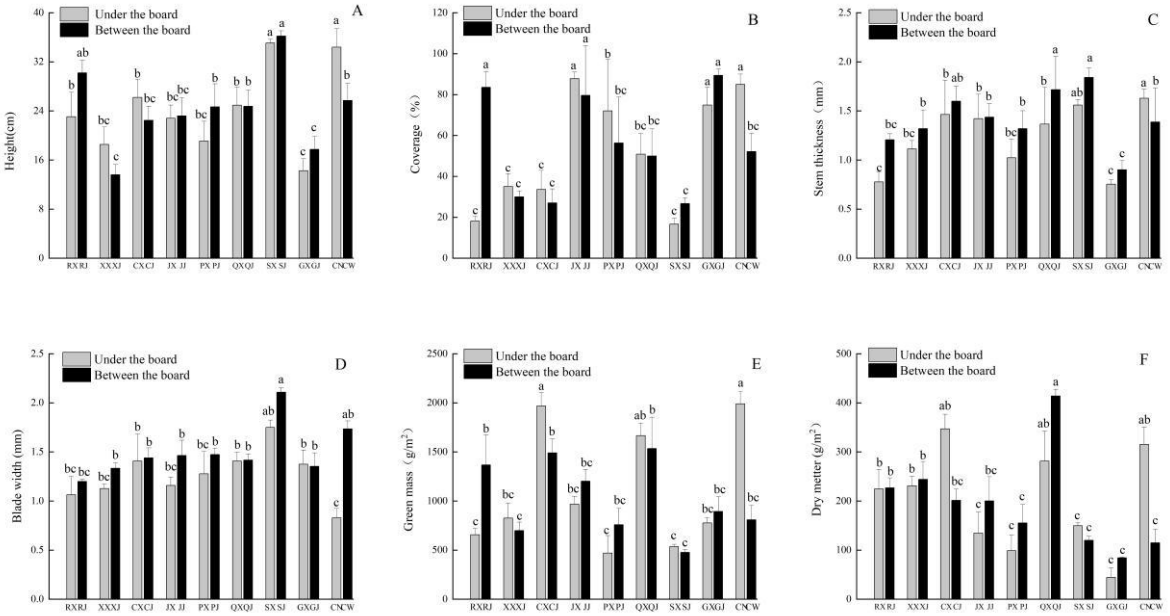

Fig. 2 - Plant Characteristics of Salicornia Communities under Different Support Structures.
(A) Height; (B) Coverage; (C) Stem thickness; (D) Blade width; (E) Fresh biomass; (F) Dry matter.

Effects of Different Support Modes on Salicornia Herbaceous Cover

As shown in Fig. 2-B, the highest cover was observed between fixed support panels (GJ) at 89.44%, followed by flexible support panels (RJ) at 83.56%. The lowest cover was recorded beneath flexible supports (RX), at merely 18.15%. Coverage differences between the inter-panel (J) and under-panel (X) regions varied across support configurations. For instance, the flat single-axis support inter-panel (PJ) coverage of 56.36% was significantly lower than its under-panel (PX) coverage of 72.06% (P<0.05)This is consistent with the findings of previous studies *(Li et al., 2024)*; the fixed bracket plate-to-plate coverage (GX) of 89.44% was significantly higher than its plate-to-plate coverage (GX) of 74.89% (P<0.05); the full-dimensional tracking bracket plate-to-plate coverage (QJ) of 50% showed no significant difference compared to its plate-to-plate coverage (QX) of 50.83% (P>0.05).This may be related to how different support types affect light shading and mechanical support strength. Research indicates that inter-row (J-shaped) supports can significantly enhance crops' photosynthetically active radiation, thereby promoting improvements in morphological indicators such as stem thickness, leaf width, and fresh biomass, though growth responses vary across different crops *(Geng et al.,2025)*.

Effect of Different Support Systems on Salicornia Stem Diameter

As illustrated in Fig. 2-C, significant variations in stem diameter characteristics were observed across Salicornia communities. The double-axis support system between panels (SJ) group exhibited the most robust stem development, with a diameter reaching 1.84 mm, while the fixed support between plates (GJ) group exhibited the lowest stem diameter at merely 0.75 mm, followed by the flexible support beneath plates (RX) group at 0.78 mm. Overall, stems between plates (J-type) consistently demonstrated superior diameter to those beneath plates (X-type), reflecting how ample light promotes stem thickening. Rotatable dual-axis tracking mounts, whilst providing ample illumination, maintain substantial spatial ventilation, thereby positively enhancing crop photosynthetic efficiency and yield *(Geng et al.,2025)*.

Effect of Different Support Systems on Salicornia Leaf Width

As shown in Fig. 2-D, significant differences in leaf width were observed among Salicornia communities under different support types. The field control (CN) group exhibited the narrowest leaf width at 0.83 mm, significantly lower than other groups ($P<0.05$). Leaf widths were generally greater between boards (J-type) than beneath boards (X-type). For instance, the double-axis support between boards (SJ) group recorded 2.11 mm, exceeding the double-axis support beneath boards (SX) group at 1.75 mm; similarly, the flexible support between boards (RJ) group measured 1.20 mm, surpassing the flexible support beneath boards (RX) group at 1.06 mm. However, in the vertical uniaxial (C) group, the leaf width under the plate (CX) at 1.41 mm was lower than that between plates (CJ) at 1.44 mm. The majority of leaf width measurements in the inter-board group were superior to those in the under-board group, further demonstrating that the spatial arrangement of supports (inter-board versus under-board) is a key determinant of light intensity and ventilation conditions.

Effect of Different Support Systems on fresh biomass of Salicornia

As illustrated in Figure 2-E, fresh biomass data reveal significant variations in biomass accumulation. The field control (CN) group exhibited the highest fresh biomass at 1990 g/m², markedly surpassing other trellis types and highlighting its growth advantage; conversely, the flat single-axis trellis under-board (PX) group recorded the lowest fresh biomass at merely 470 g/m². Fresh biomass under inter-panel (J-type) supports generally exceeded that under panels (X-type). For instance, the flexible support inter-panel (RJ) group recorded 1367.33 g/m², significantly higher than the flexible support under-panel (RX) group at 656 g/m² (P<0.05). This indicates flexible supports maintain adequate light penetration while providing moderate mechanical support. The dual-axis support(S) group exhibited unusual results, with inter-panel (SJ) fresh biomass (477.33 g/m²) being lower than under-panel (SX) fresh biomass (536.67 g/m²).

Effect of Different Support Systems on Salicornia dry matter

As illustrated in Fig. 2-F, dry matter accumulation exhibited significant variation across support types: the inter-panel (QJ) configuration under the full-dimensional support system yielded the highest dry matter at 414 g/m². while the lowest dry matter was recorded under fixed support boards (GX) at merely 44.33 g/m². Similarly, the dry matter between fixed support boards (GJ) was relatively low at 84.33 g/m². The pattern of dry matter variation between boards (J-type) and beneath boards (X-type) was not pronounced. Fresh biomass under flexible support plates (RJ) at 227 g/m² exceeded that under flexible support plates (RX) at 224.67 g/m², while fresh biomass between vertical single-axis support plates (CJ) at 201.33 g/m² was significantly lower than that under vertical single-axis plates (CX) at 347 g/m² ($P<0.05$). This may stem from the fundamental

mechanism by which canopy structure influences light utilisation. Previous studies indicate that increases in canopy volume or leaf area directly enhance aboveground biomass and improve overall photosynthetic efficiency by optimising light distribution *(Negar et al., 2024; Zhai et al., 2024),* further validating the regulatory role of support layout in capturing photosynthetic resources.

Effects of Different Support Structures on Soil Characteristics in Salicornia Communities within Photovoltaic Fields

Effects of Eight Photovoltaic Panel Support Structures on Soil pH in Salicornia Communities

Soil pH, electrical conductivity, and salt ion content serve as crucial indicators for assessing soil salinisation levels, significantly influencing the formation and transformation of substances within the soil, microbial activity, and various physiological and biochemical processes *(Li et al.,2018)*. As shown in Fig. 3-A, the analysis of soil pH across the eight support configurations reveals no significant variation in pH values within the Salicornia communities. Differences between areas beneath and between panels were non-significant (P>0.05). The highest pH value (9.56) was recorded beneath the vertical single-axis support (CX), while the lowest pH (8.80) was observed beneath the fixed support (GX). This may be attributed to the relatively concentrated positioning of photovoltaic arrays within the study plots, resulting in low soil spatial heterogeneity and minimal pH differences between treatments. It also suggests that salt stress exerts little influence on Salicornia growth, whereas only extremely high pH levels (alkaline stress) inhibit its development *(Liu et al., 2010)*.

Impact of Eight Photovoltaic Panel Support Configurations on Soil Conductivity

As illustrated in Fig. 3-B, analysis of conductivity across the eight support configurations reveals that the seasonally adjustable support system exhibited the highest inter-panel conductivity (JJ), reaching 2.34 ms/cm. The lowest conductivity was observed in the off-site control group (CW), at merely 1.31 ms/cm. The conductivity beneath the panels (X) for all eight support types was lower than that between panels (J). The conductivity of the in-field control group (CN) at 1.54 ms/cm was higher than that of the out-of-field control group (CW) at 1.31 ms/cm.

Effect of Eight Photovoltaic Panel Support Configurations on Total Soil Base Content

As shown in Fig. 3-C, the fixed support (G), inclined single-axis support (X), and dual-axis tracking support (S) groups exhibited higher total soil base content, with no significant difference between above-panel and below-panel base levels (P>0.05). The fixed-mount panel-under (GX) group exhibited the highest soil total base content at 5.65 g/kg. The lowest soil total base content was observed between panels (QJ) under the full-axis tracking support, at merely 4.10 g/kg. For the flexible support (R) and flat single-axis support (P) groups, soil total base content between panels was lower than beneath panels; for the remaining groups, soil total base content between panels exceeded that beneath panels. In this study, the water-soluble salt content in the topsoil layer of the high-cover area with Salicornia herbacea was relatively high. This may be attributed to Salicornia herbacea being an annual halophyte that absorbs soil salts during its growth period. During the growing season, it readily produces leaf litter, which, upon decomposition, returns a substantial amount of salts to the topsoil, thereby increasing the water-soluble salt content *(Yang et al.,2018)*.

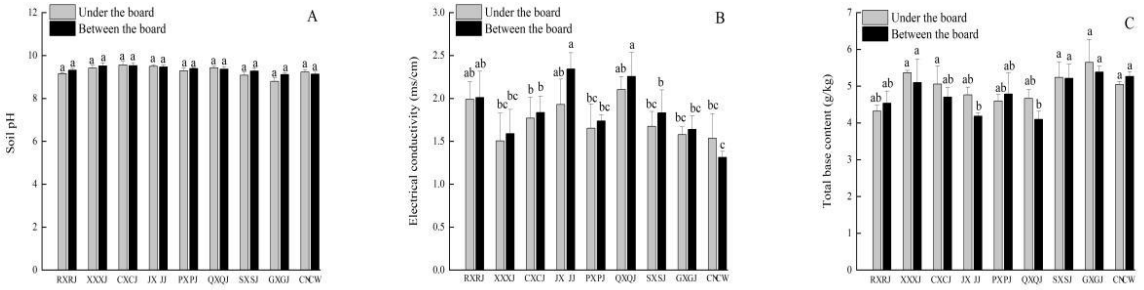

Fig. 3 - Effects of Different Support Structures on Soil Characteristics in Salicornia Communities within Photovoltaic Fields. (A) Soil pH; (B) Electrical conductivity; (C) Soil organic carbon.

Effects of Eight Photovoltaic Panel Support Structures on Soil Nutrient Content

Soil nutrients constitute the primary source of plant nutrition within grassland ecosystems, playing a crucial role in plant growth, distribution, and community composition, whilst also being influenced by vegetation succession and seasonal variations *(Elbasiouny et al., 2022)*.

During the dry season, lower soil temperatures and moisture levels constrain plant activity and microbial processes within the soil, thereby affecting the rates of organic matter decomposition and nutrient mineralization *(Zhou et al., 2022)*. As shown in Table 2, with the exception of the flat single-axis support (P) and flexible support (R) configurations, all other arrangements exhibited higher soil organic carbon content between photovoltaic panels than beneath them. This may be attributed to the higher above-ground biomass between panels, where microbial decomposition of litter and dead roots results in greater soil organic matter content compared to beneath the panels *(Wang et al., 2016).* Among the eight support types, the fixed support (G) group exhibited the highest soil organic carbon content, with combined inter-panel and under-panel organic carbon reaching 34.96%. The full-tracking support (Q) group recorded the lowest soil organic carbon content at 26.80%. Within the fixed support category, the inter-panel soil organic carbon content (GJ) was highest at 17.89%. This may stem from the fact that off-site habitats, unimpeded by photovoltaic panels, harbour longer-established natural grasslands with substantial above-ground biomass. Decaying plant residues and fallen leaves contribute to significant soil carbon levels, with organic matter primarily derived from vegetation-generated litter and decomposing roots – a process closely linked to vegetation restoration duration *(He et al., 2022; Wang et al., 2020).*

The inclined uniaxial support (X) group exhibited higher soil total nitrogen content, with inter-panel and sub-panel values reaching 1.70 g/kg; the vertical uniaxial (C) group recorded the lowest at merely 0.94 g/kg. Among these, the inter-panel soil (XJ) within the inclined uniaxial support group displayed the highest total nitrogen content at 0.99 g/kg. The highest soil total phosphorus content was observed in the fixed support (G) group at 0.67 g/kg; the lowest values were recorded in the vertical uniaxial (C) and full-dimensional tracking support (Q) groups at 0.55 g/kg. The dual-axis tracking support (S) group exhibited the highest soil total potassium content between and beneath the panels at 44.36 mg/kg, while the full-dimensional tracking support (Q) group had the lowest at 37.07 mg/kg; while the inter-panel soil (GJ) of the fixed support system recorded the highest inter-panel content at 22.52 mg/kg. Soil organic carbon, total nitrogen, total phosphorus, and total potassium concentrations in off-site habitats exceeded those in inter-panel and under-panel habitats. This disparity may stem from the microclimate influence of the photovoltaic power station, where accelerated plant growth in inter-panel and under-panel habitats necessitates greater soil nutrient uptake to sustain autotrophic requirements *(Hao et al.,2025)*.

Table 2

Analysis of Soil Nutrient Content under Eight Types of Photovoltaic Mounting Scenarios in Solar Farm Areas

	Soil organic carbon (%)	Total nitrogen (g/kg)	Total phosphorus (g/kg)	Total potassium (mg/kg)
RX	17.72a	0.71ab	0.30ab	19.79b
RJ	13.98c	0.61b	0.29ab	20.50ab
XX	15.48b	0.71ab	0.27b	18.69bc
XJ	17.04ab	0.99a	0.30ab	20.61ab
CX	15.19bc	0.44c	0.28b	17.83c
CJ	16.77ab	0.50bc	0.27b	20.51ab
JX	13.27c	0.57b	0.29ab	19.48b
JJ	14.79bc	0.81ab	0.29ab	19.62b
PX	15.98abc	0.48c	0.32ab	19.27b
PJ	18.16ab	0.71ab	0.31ab	20.09abc
QX	13.03c	0.60b	0.27b	18.44bc
QJ	13.77c	0.63b	0.28b	18.63bc
SX	14.64bc	0.72ab	0.26b	21.92a
SJ	16.16abc	0.63b	0.28b	22.44a
GX	17.07ab	0.61b	0.36a	19.41b
GJ	17.89a	0.46c	0.31ab	22.52a
CN	15.59b	0.57b	0.29ab	21.12ab
CW	16.63ab	0.51bc	0.28b	18.83bc

Correlation Analysis of Grass-Soil Interface Factors Across Eight Support Structures in Photovoltaic Fields

As illustrated in Fig. 4, both the horizontal and vertical axes of the Pearson correlation coefficient plot represent individual indicators, with colour intensity denoting the magnitude of the correlation coefficient between two indicators. Colours closer to red (coefficients approaching 1) indicate stronger positive correlations; closer to white denote weaker correlations; and closer to blue signify stronger negative correlations. At $P \leq 0.05$, community cover showed significant positive correlations with soil total nitrogen and total phosphorus; dry matter exhibited significant positive correlation with soil pH, and significant negative correlations with soil total base cation content, total nitrogen, and total phosphorus. Soil pH also showed a significant positive correlation with stem diameter and fresh biomass. Community height exhibited a significant negative correlation with soil total nitrogen and total phosphorus. At $P \leq 0.01$, height showed a highly significant positive correlation with stem diameter; stem diameter exhibited a highly significant negative correlation with total nitrogen and total phosphorus.

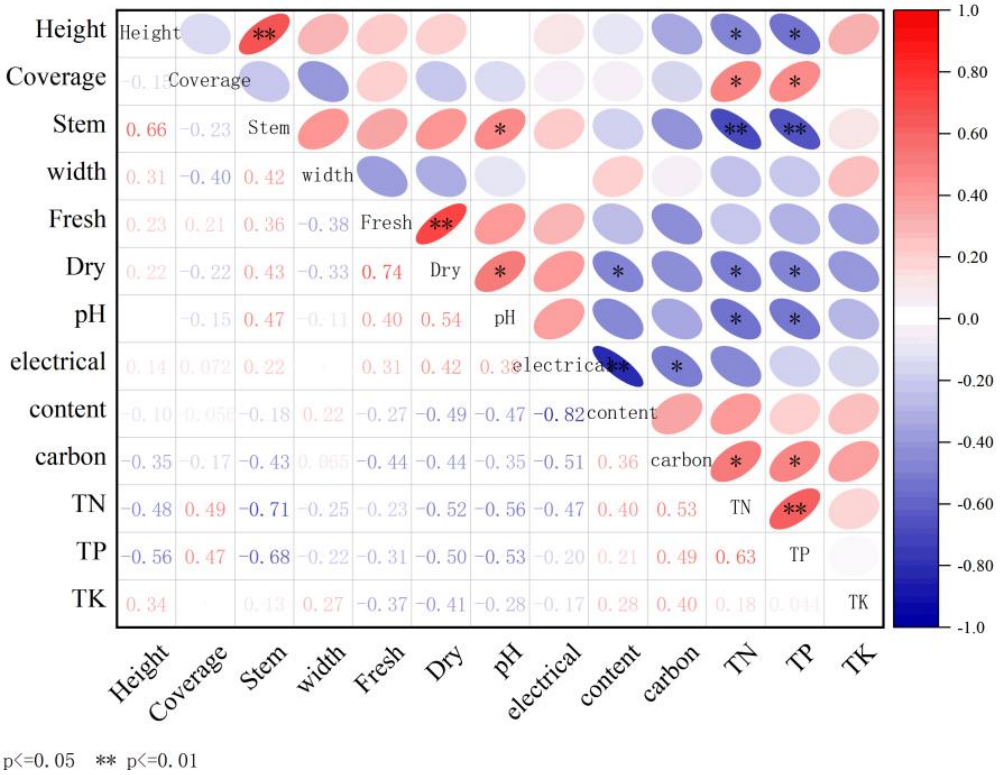

Fig. 4 - Correlation Analysis of Various Parameters in Photovoltaic Fields

Stem – Stem thickness; width – Blade width; Fresh – fresh biomass; Dry – dry matter; electrical – electrical conductivity; content – Total base content; carbon – Soil organic carbon; TN – Total nitrogen; TP – Total phosphorus; TK– Total potassium

Comprehensive Evaluation of Membership Functions for Grass-Soil Interface Indicators Across Eight Support Structures in the Photovoltaic Field

As individual indicators cannot accurately reflect the impact of the eight support structures on Salicornia and soil parameters within the national photovoltaic base, membership functions were employed. Higher membership function values indicate lesser adverse effects of the supports on the grassland. Analysis of changes in the overall evaluation D-value (Table 3) indicates that the S group exhibited the most favourable Salicornia community growth, with a combined D-value of 1.30 for both above- and below-panel areas, followed by the C group at 1.14. The on-site control group CN demonstrated significantly superior Salicornia growth compared to the off-site control group CW ($P<0.05$). The dual-axis tracking mount maintains adequate support while avoiding excessive mechanical constraints, thereby balancing light utilisation advantages with root system expansion space. This conclusion aligns with recent empirical research on the impact of photovoltaic power stations in desert regions of the Qinghai-Tibet Plateau upon vegetation-soil systems *(Hao et al., 2025)*.

Table3

Functional values of various indicators for photovoltaic fields

Bracket mode	Comprehensive Evaluation D Value	Sorting
RX	0.32	16
RJ	0.51	8
XX	0.41	14
XJ	0.43	13
CX	0.56	6
CJ	0.58	4
JX	0.47	10
JJ	0.50	9
PX	0.29	17
PJ	0.45	11
QX	0.52	7
QJ	0.57	5
SX	0.62	3
SJ	0.68	1
GX	0.13	18
GJ	0.33	15
CN	0.63	2
CW	0.43	12

CONCLUSIONS

This study demonstrates that the type and layout of photovoltaic supports significantly influence the growth of Salicornia herbacea and soil properties in saline-alkali land. Among the support types, the inter-panel layout (SJ) of dual-axis tracking supports yielded the best performance in plant height, stem diameter, leaf width, fresh biomass, and dry matter, achieving the highest comprehensive evaluation D-value (1.30), indicating its strongest positive effect on the grassland ecosystem. The inter-panel layout of flexible supports also enhanced biomass. Regarding soil properties, all eight support configurations showed no significant effect on pH. However, soil electrical conductivity was generally higher between panels than beneath them, with total base cation content highest beneath fixed supports. Except for flat single-axis and flexible supports, soil organic carbon content was generally higher between panels than beneath them. Differences in nutrients such as total nitrogen, phosphorus, and potassium were observed across support types. In summary, the inter-panel layout of dual-axis tracking supports maximises light utilisation, increases Salicornia herbacea yield, and promotes soil organic matter recovery. It is recommended that dual-axis tracking supports be prioritised for photovoltaic-agriculture synergistic utilisation in saline-alkali grassland. Additionally, salinity in the area beneath the panels should be regulated through irrigation or soil conditioners to achieve synergistic yield increases and ecological restoration for both the photovoltaic system and halophytic vegetation.

ACKNOWLEDGEMENT

This research was funded by the Daqing new energy field “unveiling the list” science and technology research project of China (Grant No. 2021BD05), Heilongjiang Provincial Science and Technology Department, the Provincial Academy Cooperation Project of China (Grant No. YS16B12).

REFERENCES

[1] Che G., Li Y., Hu Y., Wang Y., Wu Y., Liu F. (2025). Mechanisms and Effects of Photovoltaic Arrays on Microclimate and Soil in the Central Yunnan Karst Desertification Region (滇中石漠化地区光伏阵列对微气候-土壤的影响机制及效应). *Journal of Soil and Water Conservation*, vol.39, no.3, pp.191-201, DOI: https://doi.org/10.13870/j.cnki.stbcxb.2025.03.010.

[2] Elbasiouny H., ElRamady H., Elbehiry F., Rajput V.D., Minkina T., Mandzhieva S. (2022). Plant Nutrition under Climate Change and Soil Carbon Sequestration (气候变化下的植物营养与土壤碳固存). *Sustainability*, vol.14, no.2, p.914, DOI: https://doi.org/10.3390/su14020914.

[3] Geng X., Zhang L., Bao E., Gong J., Cao K., Zhang J. (2025). Effects of different photovoltaic array structures on shading, light environment and wheat yield (不同光伏阵列结构对遮阴、光环境及小麦产量的影响). *Transactions of the Chinese Society for Agricultural Engineering*, vol.41, no.15, pp.227-235, DOI: https://doi.org/10.11975/j.issn.1002-6819.202406011.

[4] Gugulothu R., Somanchi N., Vilasagarapu D., Banoth H. (2015). Solar Water Distillation Using Three Different Phase Change Materials (使用三种不同相变材料的太阳能水蒸馏). *Materials Today: Proceedings*, vol.2, no.4-5, pp.1868-1875, DOI: https://doi.org/10.1016/j.matpr.2015.07.137.

[5] Hao X., Yu H., Wu X., Feng T., Wang C., Tian L., ..., Wang P. (2025). Impact of typical photovoltaic power station construction on vegetation attributes and soil properties in desert areas of the Qinghai-Tibet Plateau (青藏高原荒漠区典型光伏电站建设对植被属性和土壤性质的影响). *Acta Ecologica Sinica*, vol.45, no.11, pp.5510-5526, DOI: https://doi.org/10.20103/j.stxb.202410092441.

[6] Hassani A., Azapagic A., Shokri N. (2020). Predicting long-term dynamics of soil salinity and sodicity on a global scale (在全球尺度上预测土壤盐分和碱度的长期动态). *Proceedings of the National Academy of Sciences of the United States of America*, vol.117, no.52, pp.33017-33027, DOI: https://doi.org/10.1073/pnas.2013771117.

[7] He Q., Chen D., Li S., Zhang F., Sun Y., Zheng J., ..., Zhao M. (2022). Changes in Plant Community Biomass and Soil Nutrients in Abandoned Farmland with Different Restoration Durations on the Northern Foothills of the Yinshan Mountains (阴山北麓不同恢复年限弃耕地植物群落生物量与土壤养分变化). *Chinese Journal of Grassland Science*, vol.44, no.10, pp.30-37, DOI: https://doi.org/10.16742/j.zgcdxb.20210143.

[8] Hu C., Zhu H., Zhang F., Wang X., Hou S., Feng W. (2024). Soil amendments reduce CH4 and CO2 but increase N2O and NH3 emissions in saline-alkali paddy fields (土壤改良剂减少盐碱稻田 CH4 和 CO2 排放但增加 N2O 和 NH3 排放). *The Science of the Total Environment*, vol.924, p.171673, DOI: https://doi.org/10.1016/j.scitotenv.2024.171673.

[9] Li Q., Xi M., Wang Q., Kong F., Li Y. (2017). Characterization of soil salinization in typical estuarine area of the Jiaozhou Bay, China (中国胶州湾典型河口区土壤盐渍化特征). *Physics and Chemistry of the Earth*, vol.103, pp.51-61, DOI: https://doi.org/10.1016/j.pce.2017.06.010.

[10] Li S. (2024). *Study on the main halophytic plants-soil feedback effects in saline-alkali grasslands of Songnen Plain (松嫩平原盐碱化草地主要盐生植物-土壤反馈效应研究)* (Master's thesis). Northeast Normal University, Changchun, China, DOI: https://doi.org/10.27011/d.cnki.gdbsu.2024.001665.

[11] Liu J., Gao B., Li X., Song J., Fan H., Wang B., Zhao K. (2010). Effects of salt-drought interaction on seed germination and seedling growth of Salicornia herbacea in different habitats (盐旱互作对不同生境盐地碱蓬种子萌发和幼苗生长的影响). *Acta Ecologica Sinica*, vol.30, no.20, pp.5485-5490, DOI: https://doi.org/10.20103/j.stxb.2010.20.009.

[12] Liu Y., Zhang R., Huang Z., Cheng Z., López-Vicente M., Ma X., Wu G. (2019). Solar photovoltaic panels significantly promote vegetation recovery by modifying the soil surface microhabitats in an arid sandy ecosystem (光伏板通过改变干旱沙地土壤微生境显著促进植被恢复). *Land Degradation & Development*, vol.30, no.18, pp.2177-2186, DOI: https://doi.org/10.1002/ldr.3408.

[13] Liu Z., Peng T., Ma S., Qi C., Song Y., Zhang C., ..., Na X. (2023). Potential benefits and risks of solar photovoltaic power plants on arid and semi-arid ecosystems: an assessment of soil microbial and plant communities (光伏电站对干旱半干旱生态系统土壤微生物和植物群落的潜在效益与风险). *Frontiers in Microbiology*, vol.14, p.1190650, DOI: https://doi.org/10.3389/fmicb.2023.1190650.

[14] Ma W., Li X., Liu S. (2018). Spatio-temporal variations of soil water content and salinity around individual Tamarix ramosissima in a semi-arid saline region of the upper Yellow River, Northwest China (西北黄河上游半干旱盐渍区多枝柽柳个体周围土壤水盐时空变化). *Journal of Arid Land*, vol.10, no.1, pp.101-114, DOI: https://doi.org/10.1007/s40333-017-0072-9.

[15] Tao C. (2023). *Study on the Effect and Mechanism of Reed, Salicornia, and Bermuda Grass Planting in Improving Coastal Clayey Saline-Alkali Soil(种植芦苇、碱蓬和狗牙根对滨海黏性盐渍土壤改良效果及机理研究)* (Master's thesis). Nanjing Agricultural University, Nanjing, China, DOI: https://doi.org/10.27244/d.cnki.gnjnu.2023.000540.

[16] Wang J., Chen Z., Chen Z., Pan Z. (2020). Responses of functional traits in Eragrostis stipa-like grass leaves to soil factors under different vegetation restoration periods in eroded red soil areas of southern China (南方侵蚀红壤区不同植被恢复期土壤因子对画眉草型草本植物叶片功能性状的响应). *Acta Ecologica Sinica*, vol.40, no.3, pp.900-909.

[17] Wang T., Wang D., Guo T., Zhang G., Zhao S., Niu H., ..., Lin H. (2016). Impact of photovoltaic power station construction on soil and vegetation (光伏电站建设对土壤和植被的影响). *Research of Soil and Water Conservation*, vol.23, no.3, pp.90-94, DOI: https://doi.org/10.13869/j.cnki.rswc.2016.03.016.

[18] Wang Z., Wang J., Gao Y., Dang X., Meng Z. (2019). Impact of photovoltaic power station construction on the ecological environment in sandy areas (光伏电站建设对沙区生态环境的影响). *Bulletin of Soil and Water Conservation*, vol.39, no.1, pp.191-196, DOI: https://doi.org/10.13961/j.cnki.stbctb.2019.01.031.

[19] Yu L., Yang J., Bu K., Liu T., Jiao Y., Li G., ..., Zhang S. (2021). Impacts of Saline-Alkali Land Improvement on Regional Climate: Process, Mechanisms, and Implications (盐碱地改良对区域气候的影响：过程、机制与启示). *Remote Sensing*, vol.13, no.17, p.3407, DOI: https://doi.org/10.3390/rs13173407.

[20] Zhai M., Wei X., Pan Z., Xu Q., Qin D., Li J., ..., Wang Z. (2024). Optimizing plant density and canopy structure to improve light use efficiency and cotton productivity: Two years of field evidence from two locations. *Industrial Crops & Products*, vol.222, p.119946, DOI: https://doi.org/10.1016/j.indcrop.2024.119946.

[21] Zhao Y., Li T., Liu J., Sun J., Zhang P. (2022). Ecological stoichiometry, salt ions and homeostasis characteristics of different types of halophytes and soils. *Frontiers in Plant Science*, vol.13, p.990246, DOI: https://doi.org/10.3389/fpls.2022.990246.

[22] Zhou W., Shen W., Li Y., Hui D. (2017). Interactive effects of temperature and moisture on composition of the soil microbial community (温度和湿度对土壤微生物群落组成的交互影响). *European Journal of Soil Science*, vol.68, no.6, pp.909-918, DOI: https://doi.org/10.1111/ejss.12488.

[23] Ziaei N., Talebi M., Sayed Tabatabaei B., Sabzalian M., Soleimani M. (2024). Intra-canopy LED lighting outperformed top LED lighting in improving tomato yield and expression of the genes responsible for lycopene, phytoene and vitamin C synthesis. *Scientific Reports*, vol.14, no.1, p.19043, DOI: https://doi.org/10.1038/s41598-024-69210-z.

[24] ***International Energy Agency Releases 2024 Renewable Energy Report (国际能源署发布《2024 年可再生能源报告》). (2024). *Energy Conservation and Environmental Protection*, no.10, pp.2-3.